VISUALIZING ELECTRON BEAM DYNAMICS AND INSTABILITIES WITH SYNCHROTRON RADIATION AT THE APS*

B. X. Yang†, A. H. Lumpkin, APS, Argonne National Laboratory, Argonne, IL 60439, U.S.A.

Abstract

The Advanced Photon Source (APS) is a third-generation hard x-ray source serving a large scientific user community. In order to characterize the high-brilliance beams, the APS diagnostics beamlines have been developed into a full photon diagnostics suite. We will describe the design and capabilities of the APS visible-light imaging line, the bend magnet x-ray pinhole camera, and a unique diagnostics undulator beamline. Their primary functions are to support APS user operations by providing information on beam sizes (20 - 100 micrometers), divergence (3 – 25 microradians), and bunch length (20 – 50 ps). Through the use of examples, we will show how these complementary imaging tools are used to visualize the electron dynamics and investigate beam instabilities. Special emphasis will be put on the use of undulator radiation, which is uniquely suitable for time-resolved imaging of electron beam with high spatial resolution and for measurements of longitudinal beam properties, such as beam energy spread and momentum compaction.

INTRODUCTION

The Advanced Photon Source is a third-generation hard x-ray source serving a large scientific user community. In order to characterize the high-brilliance beams, a bend magnet radiation beamline (35BM) and an insertion device beamline (35ID) were allocated during the construction of the APS for electron beam diagnostics [1-5]. In the past ten years, these APS diagnostics beamlines have been developed into a full photon diagnostics suite.

Figure 1 shows a floor plan of the current devices in the diagnostics beamlines. An x-ray pinhole camera line is installed in the front end to provide beam size measurements (resolution ~ 22 μm) at video rate (30 Hz).

A specially designed undulator, with many short magnetic periods and low field error, is used as the x-ray source in the insertion device beamline.

Optical synchrotron radiation (OSR) was used for emittance measurements during commissioning of the storage ring. But its resolution fell short as the electron beam size continued to decrease. Currently, the OSR line is used solely for time-resolved beam imaging.

X-RAY PINHOLE CAMERA

The APS storage ring x-ray pinhole camera consists of an adjustable x-ray pinhole (a set of tungsten blades), a aluminum vacuum window (10 mm thick), a YAG scintillator screen and a CCD camera with imaging optics. A VME-based digitizer processes the video in real time and calculated the beam size at 30 Hz. The beam size has been archived since 1997 (Figure 2). In 1995, when the storage ring was being commissioned and was running under 20 mA, an OSR camera was used to monitor the beam size at an rms resolution of ~60 μm. As the stored beam current gradually increased to 100 mA, the pick-up mirror distorted and the imaging resolution worsened. An x-ray pinhole camera was implemented in 1996 and was continuously improved up to 1999, with a final resolution of 22 μm.

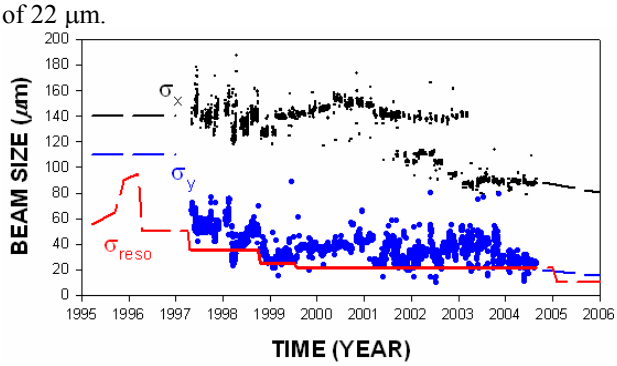

Figure 2: The rms electron beam sizes observed at the APS 35-BM bend magnet source, and the imaging resolution from 1997 to 2004.

The horizontal beam size remained ~140 μm till 2001, when a low-emittance lattice was tested [6]. Eventually, the lattice completely replaced the original design lattice by 2003, and the horizontal beam size continues to decline over the past few years. The vertical beam size, started from the design value of 110 μm, continued to

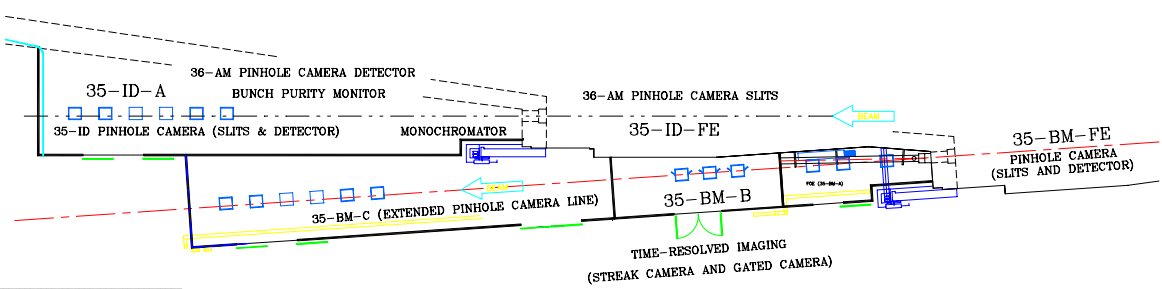

Figure 1: Floor plan of the APS Diagnostics Beamlines.

*Work supported by the U.S. Dept. of Energy, Office of Basic Energy Sciences, under contract number W-31-109-ENG-38.

†bxyang@aps.anl.gov

reduce. In 2004, the vertical beam sizes consistently remain under 35 μm.

Recording the measured beam sizes continuously (data logging) is not only used to monitor proper operation of the storage ring but also to find tell-tale signs that subtle instability is present [7].

OSR MEASUREMENTS

Beamline Design and Experiment Setup

Figure 3 shows a schematic of the APS storage ring OSR imaging line. The OSR light is picked up by a water-cooled mirror behind a water-cooled copper tube, which blocks the hottest part of the bend magnet radiation fan. A spherical mirror is used to form an image at the end of the transport line (path length ~ 47 m), located in an optics lab on the experimental floor. Along with beam splitters and secondary optics, a Hamamatsu C5680 streak camera a Quik05 gated intensified camera are used for time-resolved imaging.

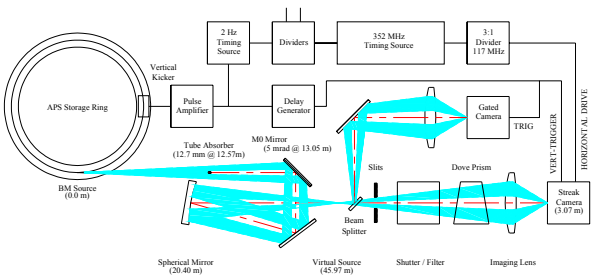

Figure 3: APS storage ring OSR imaging setup.

In a streak tube, photoelectrons generated by an OSR light pulse are accelerated and focused on to a micro-channel plate (MCP), and the intensified electronic image is converted to light by a phosphor screen. When a vertical electric field ramps rapidly to deflect the electron beam before it strikes the MCP, a streak image forms on the screen. The streak image is a projection of the bunch's electron density at an angle θ_y from its direction of travel,

$$\tan\theta_y = \frac{y_{FS}}{c \cdot t_{FS}}, \qquad (1)$$

where t_{FS} and y_{FS} are the full-scale time and displacement over the entire video screen, respectively. When this tangent ratio is well above the bunch's aspect ratio ($\tan\theta_y >> \sigma_y/\sigma_z$), the streak camera is said to be in top-view mode. Conversely, the streak camera is said to be in front-view mode when $\tan\theta_y << \sigma_y/\sigma_z$. When the side view of the electron bunch is of interest, we add an image rotation optic, such as a dove prism or a set of mirrors, to rotate images in the transverse plane (Fig. 3). Note that this definition of views depends on the optical magnification (Δx, Δy), streak sweep range, and the electron beam's aspect ratio.

Bunch Length and Phase Measurements

Top-view mode is normally employed in the APS to provide bunch-timing information to users [8]. The bunch-length data and bunch profiles are also available to users on request. This view is also appropriate for visualizing longitudinal instabilities. Figure 4 shows a multibunch instability observed during machine studies when the bunches' rf phase oscillations are driven by a higher order mode of the rf cavity.

Recently several approaches for generating short bunches are under investigation at the APS. Figure 5 shows one of the techniques being studied, where the phase of rf cavity is modulated at twice the synchrotron frequency to force bunches into a quadrupole shape oscillation [9].

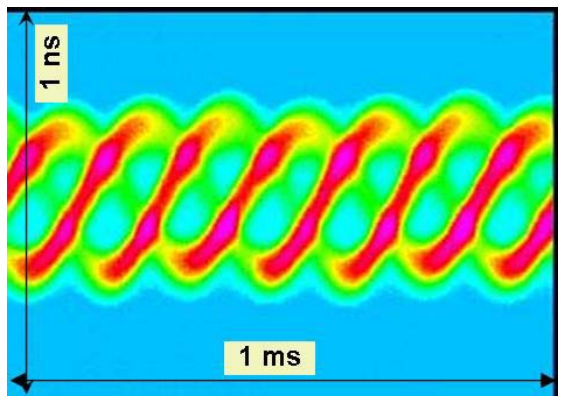

Figure 4: Dual-sweep streak image of a HOM multi-bunch instability observed in machine studies (7/4/2002). The vertical axis is the fast time scale (full scale = 1 ns) and the horizontal axis is the slow axis (full scale = 1 ms).

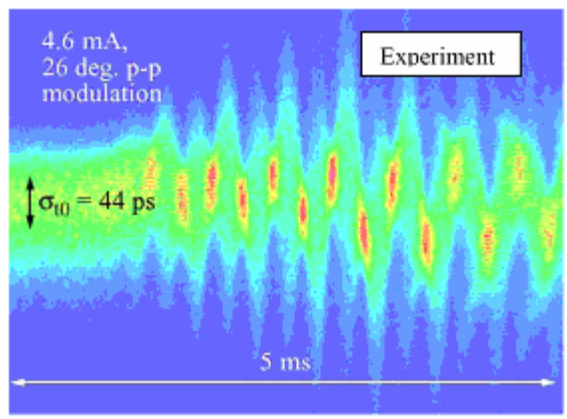

Fig. 5: Streak images of a longitudinal shape oscillation.

Bunch-by-Bunch Transverse Imaging

The rf bucket spacing of the APS storage ring, 2.84 ns, is too short for fast video cameras to distinguish. However, since the bunch length (~ 8 mm) is well below the bucket spacing (85 cm), a streak camera operating in front-view mode captures images of consecutive bunches and arranges them separately in a column. When the sweep in the orthogonal direction (dual-sweep) is also enabled, we can study the bunch motion turn after turn [10]. Figure 6 shows such an image for a bunch-train instability observed in the APS storage ring during machine studies. Twenty 1-mA bunches were filled in consecutive buckets. The wake field coupled the adjacent

0-7803-8859-3/05/$20.00 ©2005 IEEE

bunches so their horizontal motion was amplified down the trains.

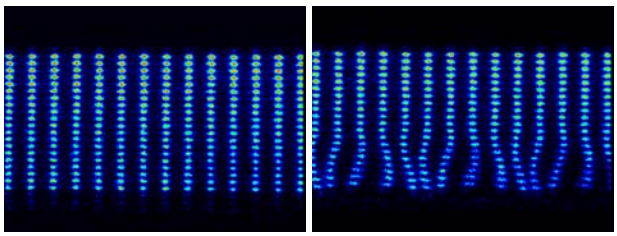

Figure 6: Dual-sweep streak images of a bunch-train instability in the APS storage ring. The vertical scale is 100 ns and the horizontal scale is 50 μs. (Left panel) stable beam, (right panel) instability occurs at low chromaticity setting.

UNDULATOR MEASUREMENTS

Undulator Beamline Design

Table 1 lists the design parameters of the APS diagnostics undulator. At and above the photon energy of the first harmonic, the x-ray beam forms a narrow cone with an rms radius of 2.7 μrad, which can be used for measuring electron beam divergence in both x and y directions. Figure 7 shows the basic setup of the beamline optics. During user operations, the undulator is set at low-power mode (total power ~ 4 W) with the first harmonic at 25 keV. A water or liquid-nitrogen (LN2) cooled thin Si(110) crystal is used to reflect monochromatic x-rays in Laue geometry. A thin YAG:Ce scintillator crystal and a CCD camera are used to read out the footprint of the x-ray beam. Since most x-ray photons pass through the thin crystal, a pinhole camera was built to image the ID source. The resolution is limited to about 40 μm due to Fresnel diffraction [4]. The images for ID beam divergence and source size are made available to users in real time.

Table 1: APS Diagnostics Undulator Design Parameters

Period	18 mm
Number of periods	198
Total length	3.56 m
Minimum gap	10.5 mm
Maximum peak magnetic field	0.27 T
Maximum K-value	0.46
First harmonic photon energy, ω_1	23.4 - 25.5 keV
RMS radiation cone angle at ω_1	2.7 - 2.6 μrad
Maximum peak power density	116 kW/mr^2
Maximum total power	0.83 kW

Electron-Beam Energy Measurements

Both the undulator field quality and the electron beam divergence affect the x-ray flux through a pinhole aperture far from the source. Thus the pinhole spectra have been used as a benchmark for the quality of both the undulator and the electron beam. However, if we open the aperture to an angular radius of $1/\gamma$, the spectrum of flux through the aperture demonstrates a sharp edge located at every

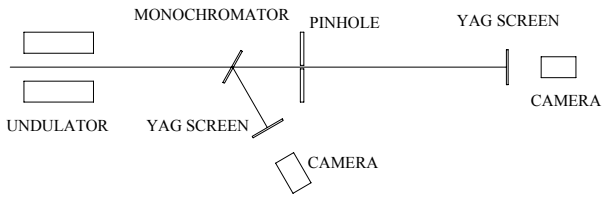

Figure 7: Sketch of undulator beamline setup.

odd harmonic with little background (Figure 8). Due to the steep slope of flux intensity changes at this edge,

$$-\frac{\Delta F}{F} \approx 2nN\frac{\Delta\omega}{\omega_1}, \qquad (1)$$

an intensity (F) measurement of moderate resolution translates into a high-resolution photon energy (ω) measurement. We have used two methods to analyze the measured spectra. In the first one, we numerically differentiate the spectra and compare them to the numerically calculated spectral derivative (Figure 8). With the second method, we fit the measure spectra with an error function with finite width and compare that with a calculated spectrum. The results of the two methods differ slightly but the second method is much faster and much more tolerant of experimental errors. From these analyses, we can extract the harmonic photon energy and electron energy spread [11, 12].

Figure 9 shows measured photon energy changes ($\Delta\omega/\omega_1$, = 2 $\Delta p/p_0$) with varying rf frequency. The slope gives the momentum compaction factor, which is otherwise difficult to obtain experimentally.

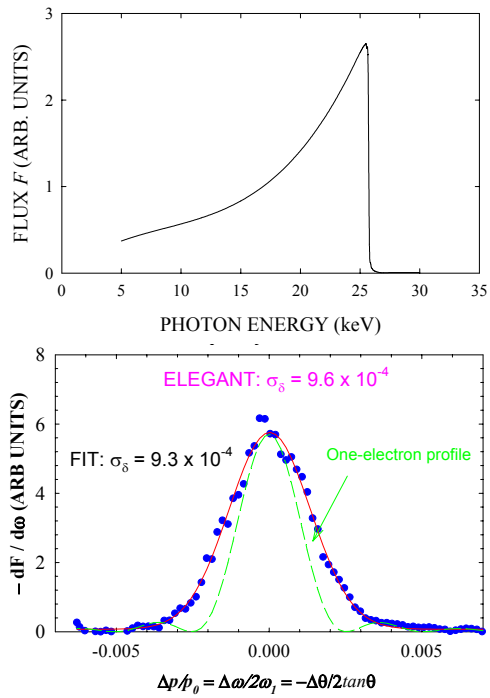

Figure 8: (Top) Calculated angle-integrated undulator spectrum for zero-emittance electron beam shows a sharp edge at the first harmonic energy. (Bottom) Negative derivative of the measured spectrum showing the effect of electron-beam energy spread.

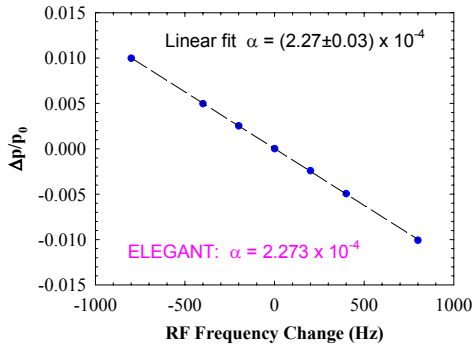

Figure 9: Measured photon energy change with storage ring rf frequency. The slope yields the momentum compaction factor of the APS storage ring.

By now we have realized that a diagnostics undulator enables us to measure the electron beam sizes and divergence at the same point, as well as beam energy centroid and spread, all in one measurement. Figure 10 shows an example of combining all these measurements. The beam emittance and the energy spread were measured as functions of the storage ring rf frequency. Due to orbit shift in the quadrupoles, the partition of longitudinal and horizontal damping can be manipulated [13]. At a lower rf frequency, the longitudinal damping is stronger (shorter bunches and lower energy spread) and the horizontal damping is weaker. Hence the horizontal emittance increased more than four-fold. When the rf frequency was further reduced, the stored beam became unstable and was quickly lost. On the higher frequency side however, the energy spread increases with the frequency and the horizontal emittance decreases.

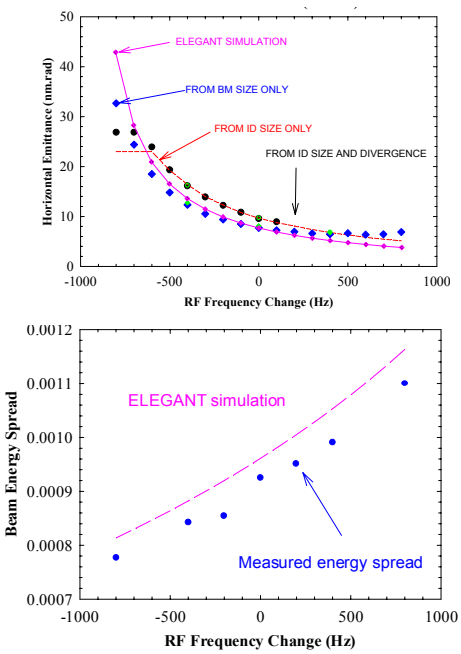

Figure 10: Measured emittance vs. rf frequency of the APS storage ring using different techniques: (Circle) from the product of ID divergence and sizes, (diamond) from the BM source size only, (dashed line) from ID source size only, and (solid line) the calculated values.

Microwave Instability

When microwave instability occurs, the electrons inside a bunch are excited internally and the charge distribution deviates from the well-damped Gaussian shape. To date, we have not been able to capture any image with non-Gaussian distribution. Instead, we looked for its signature in a time-averaged property. The energy spread increases dramatically above the threshold of microwave instability. In Figure 11, two microwave instability thresholds can be seen in the data set with 9.5 MV rf gap voltage, likely due to coupling to two different longitudinal modes [13].

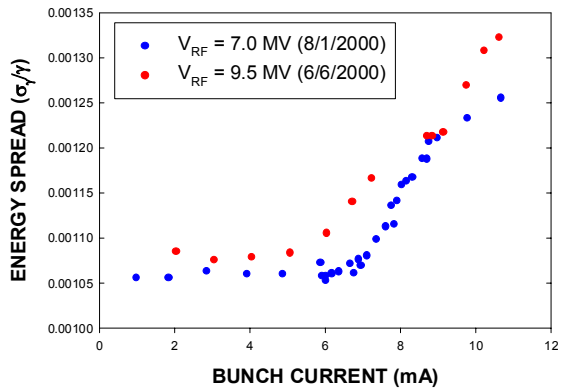

Figure 11: Measured electron beam energy spread (undulator data) as a function of stored current. (Lower curve) rf gap voltage is 7.0 MV; (Upper curve) rf gap voltage is 9.5 MV.

KICKER-INDUCED BEAM MOTION

A common technique to study beam dynamics is to kick a stored beam in a circular accelerator and observe its subsequent motion. We have used the technique with a gated intensified camera and a programmable delay to measure damping behavior using OSR [10]. Until recently, the limited resolution of OSR imaging and low flux from the bend magnet source prevented us from studying the dynamics in the vertical direction. With the commissioning of a cryogenically cooled silicon monochromator on the undulator line, we finally have a tool for mA-bunch single-turn imaging at a resolution comparable to the vertical beam size.

Figure 12 shows sample images taken with 3.5 mA stored beam at a single turn, before and 80 turns after a vertical kicker was fired. From each image, a horizontally integrated profile can be calculated. In Figure 12, we also plot over 500 such profiles in a map: the horizontal axis is the delay time, from -10 μs to 5 ms (~ log scale), the vertical axis is in μrad (full scale 100 μrad), the profile intensities are color coded at each point. We can see that, from the time of the vertical kick, the beam moves away from its initial, equilibrium position, goes into betatron oscillation, gradually broadens, and finally damps down. The rms height can be plotted against the delay time from the kicker pulse (Figure 13), and damping time can be derived from fitting the data set. We observed a shorter apparent damping time in the vertical direction (when

excited by a vertical kicker) than in the horizontal direction (when excited by a horizontal kicker). The reason for the difference is not clear, although vertical coupling should be an important factor. We also note that, in the first several ms after the kick, all degrees of freedom of the electron are important in describing its motion, as can be seen from a side-view image taken around the 80th turn after the kicker pulse [14].

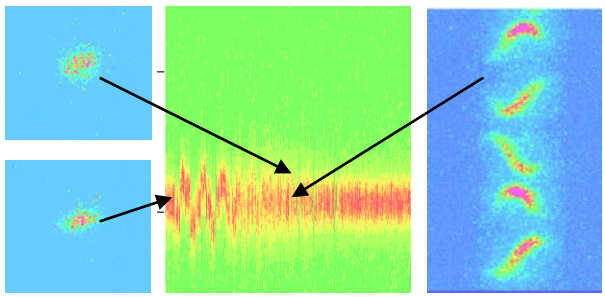

Figure 12: (Left) Single-turn undulator monochromatic x-ray imaging data from a 3.5 mA bunch: (Lower left) front-view image before vertical kicker pulse; (Upper left) front-view image 80 turns after kicker pulse. (Middle) 500 horizontally integrated intensity profile from delay time = -10 μs to 36 ms (time scale is not uniform, ~ logarithmic). (Right) Streak camera side-view image around the 80th turn.

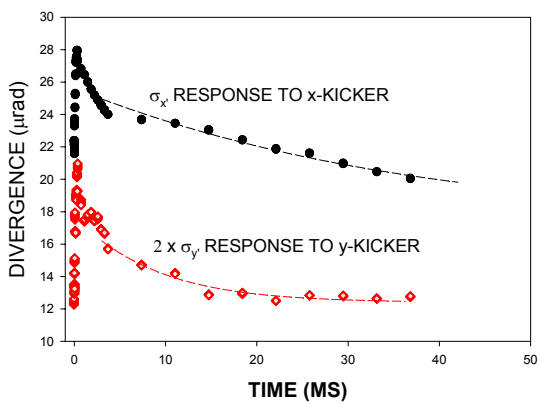

Figure 13: Measured single-turn rms undulator x-ray beam divergence as a function of time after a kicker is applied: (circles) horizontal divergence after a horizontal kick; (diamond) vertical divergence after a vertical kick.

SUMMARY AND DISCUSSION

Synchrotron radiation is an indispensable tool to provide beam dynamic information without disturbing the beam in a circular accelerator. We presented examples of visualizing beam dynamic behavior using time-resolved imaging with optical and x-ray synchrotron radiation. We also showed that an undulator is a unique tool for studying electron beam dynamics noninterceptively.

ACKNOWLEDGMENT

We would like to thank J. Galayda (now at LCLS), G. Decker, and O. Singh for their support for the APS diagnostics beamlines, F. Lenkszus, R. Laird, E. Rotela, and S. Sharma, for excellent technical support, A. Barcikowski, B. Rusthoven, and T. Buffington for their design support, and last but not the least, M. Borland and L. Emery for many night shifts taking data.

REFERENCES

[1] B.X. Yang and A.H. Lumpkin, "The Planned Photon Diagnostics Beamlines at the Advanced Photon Source," BIW'94, Vancouver, AIP Conf. Proc. 333, 252 (1995)

[2] B.X. Yang and A.H. Lumpkin, "Status of the APS Diagnostics Undulator Beamline," PAC'97, Vancouver, May 1997, p. 2137, www.jacow.org.

[3] B.X. Yang et al., "Particle-Beam Profiling Techniques on the APS Storage Ring," BIW'96, Argonne, AIP Conf. Proc. 390, p. 491.

[4] B.X. Yang and A. Lumpkin, "Simultaneous Measurements of Electron Beam Size and Divergence with an Undulator," PAC 99, p. 2161, http://www.jacow.org.

[6] L. Emery and M. Borland, "Upgrade Opportunities at the Advanced Photon Source Made Possible by Top-Up Operations," EPAC'02, p218, www.jacow.org.

[7] A.H. Lumpkin, L. Emery and B.X. Yang, "Observations of Effective Transverse Beam-Size Instabilities for a High Current per Bunch Fill Pattern in the APS Storage Ring," PAC'97, Vancouver, May 1997, p. 2137, http://www.jacow.org.

[8] A.H. Lumpkin, F. Sakamoto, and B.X. Yang, "Dual-Sweep Streak Camera Measurements of the APS User Beams," these proceedings.

[9] G. Decker, and N. Sereno, "Transient Generation of Short Pulses in the APS Storage Ring," these proceedings.

[10] B.X. Yang et al., "Characterizing Transverse Beam Dynamics at the APS Storage Ring Using a Dual-Sweep Streak Camera," BIW'98, Stanford, AIP Conf. Proc. 451, p. 229.

[11] B.X. Yang, L. Emery, and M. Borland, "High Accuracy Momentum Compaction Measurement for the APS Storage Ring with Undulator Radiation," BIW'00, Boston, May 2000, AIP Proc. 546, p. 234.

[12] B.X. Yang, and J. Xu, "Measurement of the APS Storage Ring Electron Beam Energy Spread Using Undulator Spectra," PAC'01, Chicago, June 2001, p. 2338, http://www.jacow.org.

[13] H. Wiedmann, *Particle Accelerator Physics*, Springer, New York, 1993.

[14] B. X. Yang et al., "Streak Camera Studies of Vertical Synchro-Betatron-Coupled Beam Motion in the APS Storage Ring," these proceedings.